ELSEVIER

Thermochimica Acta 260 (1995) 29–43

thermochimica acta

Oxygen potential and phase equilibria in the $Te–Sb_2O_3–Sb_2O_4$ pseudoternary part of the Sb–Te–O system at elevated temperatures

B. Onderka, J. Wypartowicz, K. Fitzner *

Institute of Metallurgy and Materials Sciences, Polish Academy of Sciences, 25 Reymonta St., 30-059 Kraków, Poland

Received 25 August 1994; accepted 22 January 1995

Abstract

Employing the electrochemical cells with the solid oxide electrolyte

Kanthal + Re, Te(l), TeO_2(s) $\| O^{-2} \|$ air, Pt

Pt + Re, Sb_2O_3(s), Sb_2O_4(s) $\| O^{-2} \|$ air, Pt

Pt + Re, Sb_2O_3(s), Sb_2O_4(s), Te(l) $\| O^{-2} \|$ air, Pt

the equilibrium oxygen potential in the pseudobinary $Te–TeO_2$, $Sb_2O_3–Sb_2O_4$ and in the $Sb_2O_3–Sb_2O_4–Te$ pseudoternary systems was determined in the temperature range 700–1173 K. In addition, the pseudobinary sections $Sb_2O_3–Te$, $Sb_2O_3–Sb_2O_4$ (1:1)–Te and $Sb_2O_4–Te$ were examined by DTA in the temperature range 500–1300 K. Using these results the evolution of the pseudoternary system with temperature can be suggested. It was found that, at 718 K, a ternary eutectic with a composition close to pure Te appears in the system. At a higher temperature, 920 K, another liquid phase is formed, which is characteristic of the ternary four-phase equilibrium $L_2 + Sb_2O_4(s) + Sb_2O_3(s) = L_1$.

Keywords: DTA; Electrochemistry; Electrolyte; Pseudobinary system; Pseudoternary system

* Corresponding author.

SSDI 0040-6031(95)02282-1

1. Introduction

Experimental information for the ternary Sb–Te–O system is scarce. Demina and coworkers [1,2] reported the pseudobinary sections Te–Sb_2O_3, Sb_2O_4–TeO_2, Sb_2O_3–Sb_2Te_3 and Sb_2O_4–Te of this ternary diagram which were established from DTA and X-ray investigations. Unfortunately, less information is available about this system at temperatures above the melting point of Sb_2Te_3. Since both Te–TeO_2 [3,4] and Sb–Sb_2O_3 [1,4] pseudobinary systems exhibit large miscibility gaps one could suppose that at high temperature two liquids also remain in equilibrium in the ternary system. However, in our previous investigation we showed that Sb–Te alloys remain in equilibrium with liquid Sb_2O_3 over the whole alloy composition range [5]. The question is then how can the field Te–TeO_2–Sb_2O_4–Sb_2O_3 be divided into tie-triangles. Simple equilibration experiments, in which a mixture of oxides $TeO_2 + Sb_2O_3$ (1:1 mole ratio) was heated at 1023 K for 24 h in an alumina crucible under an inert gas atmosphere, showed that the resulting mixture is $Te + Sb_2O_4$. Thus the quaternary field should be divided into two tie-triangles: Te–Sb_2O_3–Sb_2O_4 and Sb_2O_4–TeO_2–Te (Fig. 1). However, due to the high temperature of decomposition of Sb_2O_4 on the one hand, and the rising pressure of tellurium and the oxides (Sb_2O_3 and TeO_2) on the other, the field of our experimental activity had to be reduced to the Te–Sb_2O_3–Sb_2O_4 pseudoternary system.

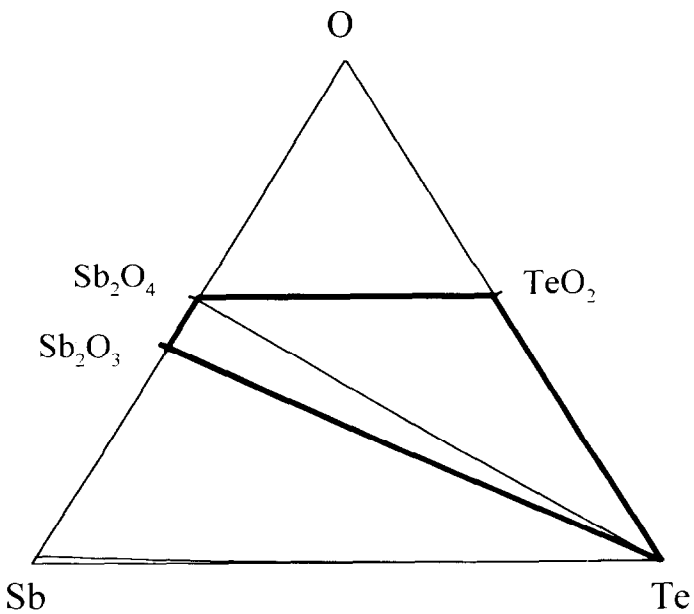

Fig. 1. Schematic representation of Sb–Te–O equilibrium diagram at temperatures above the melting point of Sb_2Te_3.

2. Experimental

2.1. Materials

Tellurium (99.9999%) was obtained from ASARCO (USA). Tellurium oxide, TeO_2, was 99.995% pure and was obtained from Johnson Matthey Electronics (USA). Antimony(III) oxide obtained from Reachim (Russia) was reagent grade and was used to prepare Sb_2O_4. This was done by heating Sb_2O_3 under a stream of oxygen at 800 K for 24 h. Formation of the required oxide was confirmed by an X-ray analysis. Solid electrolyte tubes, closed at one end, and made of either calcia- or yttria-stabilized zirconia, diameter 8/5 mm or 12/8 mm (outside/inside diameter), were obtained from Friatec AG, Div. Frialit-Degussit (Germany).

2.2. Oxygen potential measurements

The experimental method and procedure have been described previously [5, 6]. A schematic representation of the cell assembly is shown in Fig. 2. The tube of solid electrolyte contained the working electrode which consisted of the proper mixture of components. The outer part of the solid electrolyte tube coated with platinum paste worked as the air reference electrode and was connected to the electric system with a platinum wire. Purified argon was allowed through the cell just above the surface of the working electrode providing an inert atmosphere inside the cell. Either platinum wire or Kanthal A-1 wire with a welded rhenium wire tip acted as an electric contact with an electrode. Rhenium wire was obtained from Alfa-Johnson Matthey (Germany).

The cell was kept in the resistance furnace within the constant temperature zone, and the sample at the bottom of the electrolyte tube was always placed in this zone. The temperature inside the cell was maintained constant within ± 1 K. After a constant temperature was reached, the cell was left overnight to attain an equilibrium state, and then EMF was recorded with a high impedance Keithley 617 potentiometer (for cell II) (USA). The temperature was cycled in a range that depended on the investigated system, and the full run was completed after about three days.

3. Results

3.1. $Te–TeO_2$ system

To check the cell performance, the Gibbs free energy of formation of solid TeO_2 was determined in the temperature range 748–898 K. Electromotive force values of the cell

$$\text{Kanthal} + \text{Re, Te(l)} + \text{TeO}_2\text{(s)} \,\|\, \text{O}^{-2} \,\|\, \text{air, Pt} \qquad \text{(I)}$$

are shown in Fig. 3, and are represented by the equation

$$E(\pm 1)/\text{mV} = 818.54(\pm 9.71) - 0.485(\pm 0.02)T \qquad (1)$$

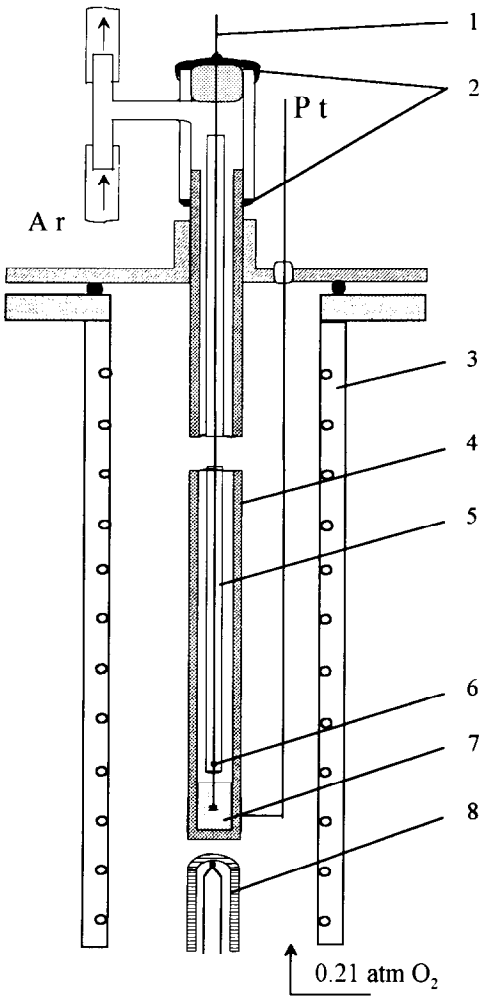

Fig. 2. Schematic diagram of the experimental arrangement: 1, Pt or Kanthal A-1 working electrode wire; 2, silicon rubber; 3, furnace; 4, solid electrolyte tube; 5, alumina shield; 6, rhenium tip; 7, sample; 8, thermocouple.

Using the relation between measured EMF and equilibrium oxygen pressure p_{O_2}

$$E = \frac{RT}{4F} \ln\left(\frac{0.21}{p_{O_2}}\right) \tag{2}$$

the Gibbs free energy change $\Delta G^0_{f,TeO_2}$ of the reaction

$$Te(l) + O_2(g) = TeO_2(s) \tag{3}$$

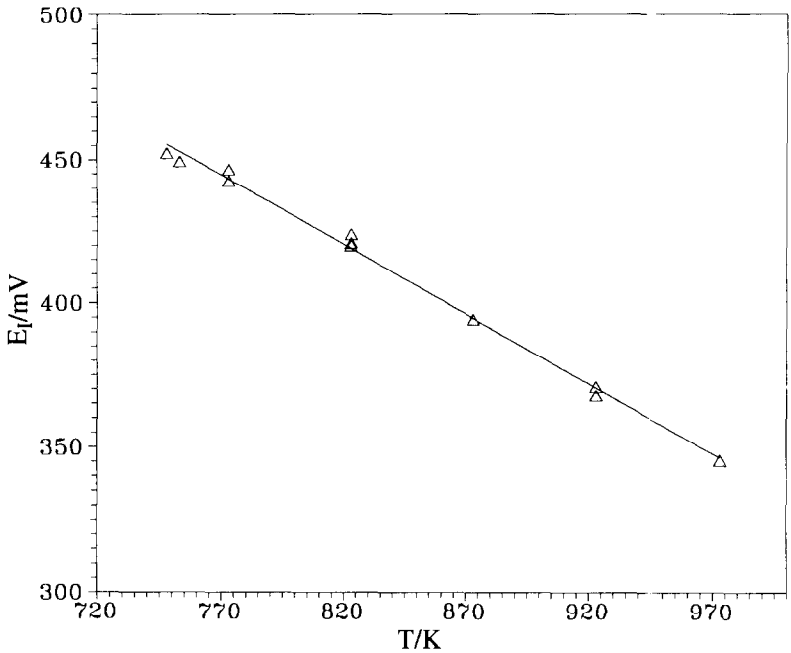

Fig. 3. E.m.f. vs. temperature dependence: Δ, this work; —, Eq. (1).

is given in the form

$$\Delta G^0_{f,TeO_2}/J\,mol^{-1} = RT\ln p_{O_2} = -4FE_I + RT\ln 0.21 \quad (4)$$
$$= -315980 + 174.4\,T(\pm 1080)$$

where R is the gas constant, T is the absolute temperature, and F is the Faraday constant. This result is in good agreement with those reported previously by Mallika and Sreedharan [7], Chatterji and Smith [8], and Otsuka and Kozuka [9] (Fig. 4). Combining Eq. (4) with our results of the oxygen activity in dilute solutions with tellurium [5], one can derive the saturation solubility equation for the Te–TeO_2 pseudobinary system

$$C_O(\text{at. \%}) = \exp\left[\frac{\Delta G^0_{f,TeO_2} - 2\Delta G^0_O(\text{in Te})}{2RT}\right] \quad (5)$$
$$= \exp\left(\frac{-7449.35}{T} + 5.80254\right)$$

where ΔG^0_O (in Te) is the Gibbs energy of dissolution of oxygen in liquid tellurium [5].

Next, accepting the monotectic temperature, determined from DTA measurements by Buketov et al. [3] (Fig. 5), the Te-rich part of binary Te–O phase diagram was calculated (Fig. 6).

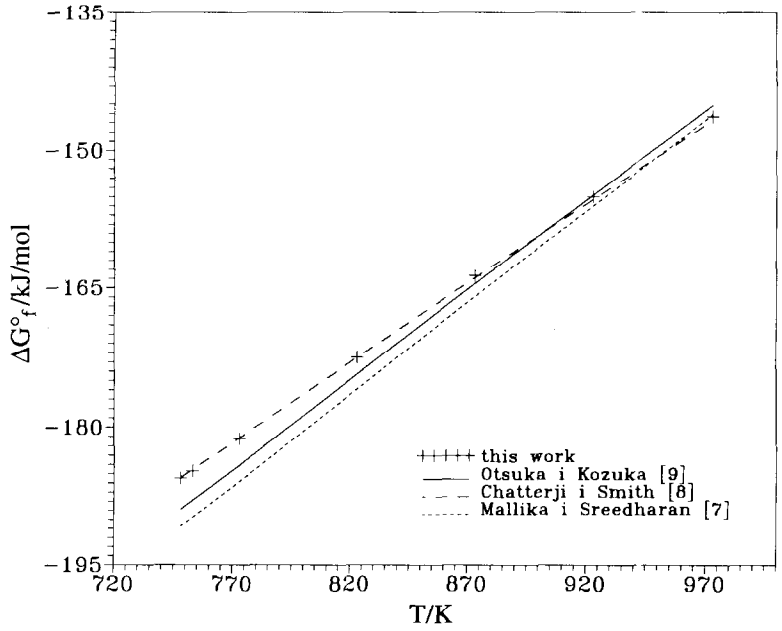

Fig. 4. Comparison of $\Delta G^{0}_{f,TeO_2}$ values obtained in this work (+) with literature data.

3.2. Sb_2O_3–Sb_2O_4 system

The cell

$$Pt + Re, Sb_2O_3(s), Sb_2O_4(s) \| O^{-2} \| \text{air, Pt} \quad \text{(II)}$$

was used to determine an equilibrium constant of the reaction

$$Sb_2O_3(s) + 0.5O_2 \rightleftharpoons Sb_2O_4(s) \quad (6)$$

Pt powder was added to the working electrode (10 mass%) in order to enhance electrical conductivity in the system. Results of e.m.f. measurements carried out in the temperature range 723–857 K are shown in Fig. 7. It was noticed that cell II had difficulties in attaining an equilibrium state.

3.3. Sb_2O_3–Sb_2O_4–Te system

Since the mutual solubility between solid oxides and liquid tellurium is negligible in the considered temperature range, the oxygen pressure is in fact determined by reaction (6), while the presence of tellurium in the working electrode enhances its conductivity and, consequently, the cell operation. The cell

$$Pt + Re, Sb_2O_3(s), Sb_2O_4(s), Te(l) \| O^{-2} \| \text{air, Pt} \quad \text{(III)}$$

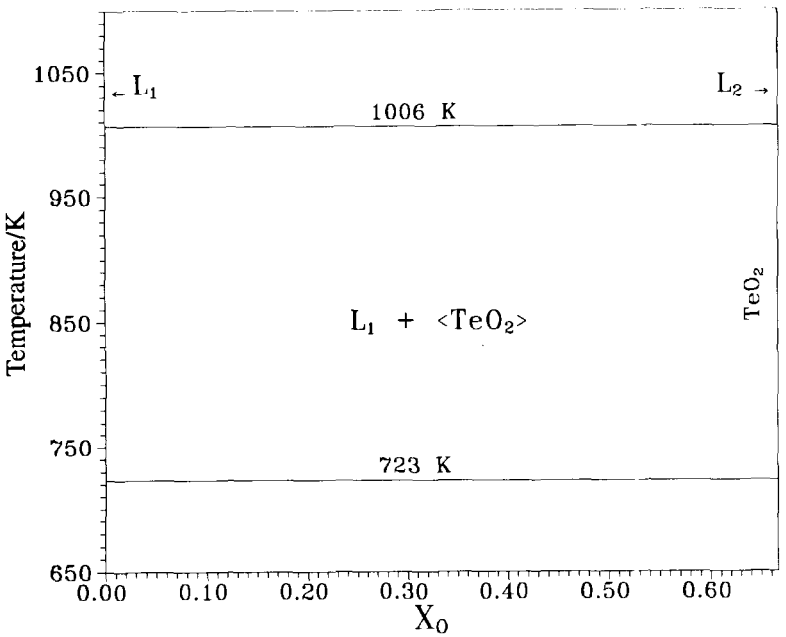

Fig. 5. Te–O phase diagram according to Buketov et al. [3].

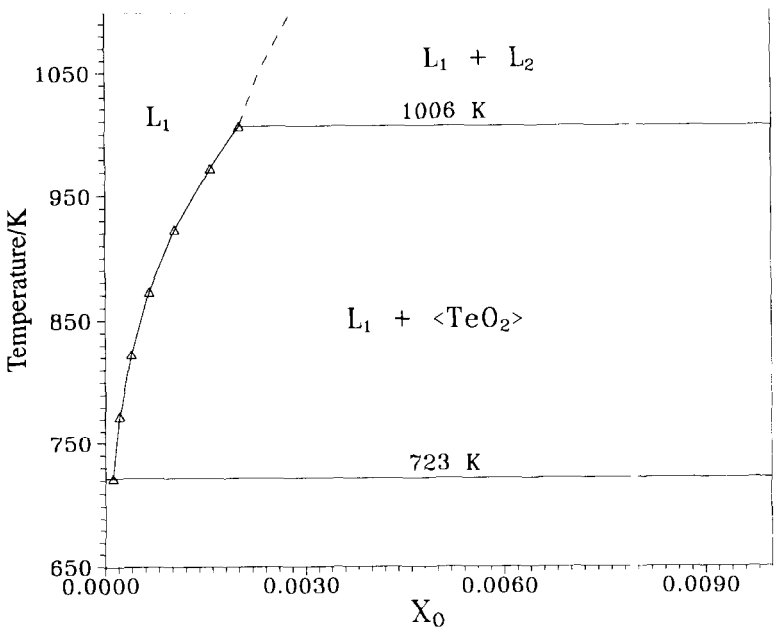

Fig. 6. Te-rich part of Te–O phase diagram calculated in this work.

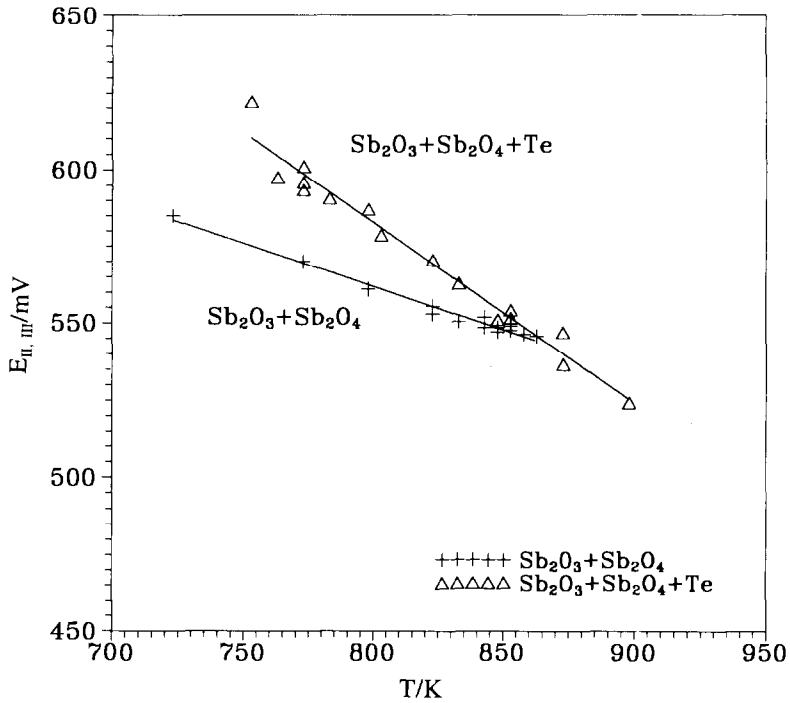

Fig. 7. E.m.f. vs. temperature plot for cells II and III.

was used to determine oxygen partial pressure in the ternary field. The e.m.f. vs. temperature dependence is shown and compared in Fig. 7 with e.m.f.s produced by cell II. At high temperature, results become identical while at low temperature a discrepancy between measured values is observed. Since at low temperature cell II attained equilibrium very slowly, and moreover, the formation of solid PtO_2 was possible [10], we assumed that equilibrium of reaction (6) is represented by the results of cell III. Obtained e.m.f. values for cells II and III were treated by the least-squares method and are represented by equations given in Table 1.

Table 1
E.m.f. values of cells II and III represented as an $E = A + BT$ function; r correlation coefficient; s mean square error

Cell no.	A	B	r	σ
II	789.717 ± 9.612	-0.28478 ± 0.01165	0.99093	1.57
III	1052.091 ± 22.215	-0.58666 ± 0.02715	0.98534	4.8

Using dependence (2) and the equilibrium constant of reaction (6), the Gibbs free energy change for this reaction was calculated

$$\Delta G^0_{(6)}/\mathrm{J\,mol^{-1}} = -2FE_{\mathrm{III}} + 0.5RT\ln 0.21 \tag{7}$$

$$= -203\,071 + 106.75T(\pm 930)$$

When this result is combined with the respective Gibbs free energy change of the reaction of formation of solid Sb_2O_3 [6], the Gibbs free energy of formation of Sb_2O_4 from pure elements is obtained

$$2Sb(s) + 2O_2(g) = Sb_2O_4(s) \tag{8}$$

$$\Delta G^0_{f,Sb_2O_4}/\mathrm{J\,mol^{-1}} = -883.070 + 339.47T \tag{9}$$

Obtained values of $\Delta G^0_{f,Sb_2O_4}$ are compared in Fig. 8 with measurements of Pankajavalli and Sreedharan [11] as well as with tabelaric values given by Barin et al. [12], Kulikov [13] and Pankratz [14].

It is obvious however, that cell III represents the $Sb_2O_3 + Sb_2O_4$ equilibrium in the presence of liquid tellurium as long as no liquid oxide phase is formed in the system. To correlate the oxygen pressure with phase equilibria at higher temperatures, more information must be obtained about the phase relations at temperatures in which this phase may appear.

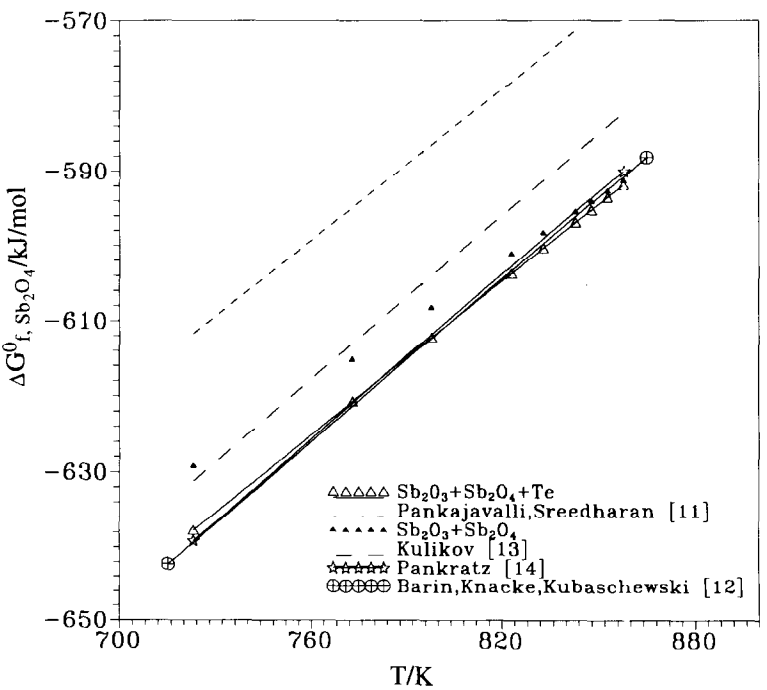

Fig. 8. Gibbs free energy of formation of solid Sb_2O_4 from pure elements.

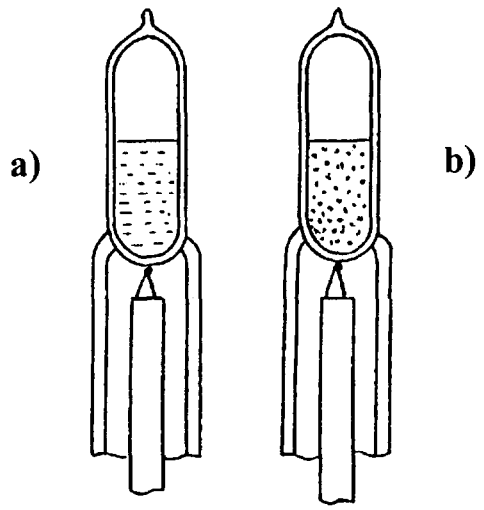

Fig. 9. Schematic construction of silica vessels used for DTA measurements: (a) sample vessel; (b) reference vessel (with Al_2O_3).

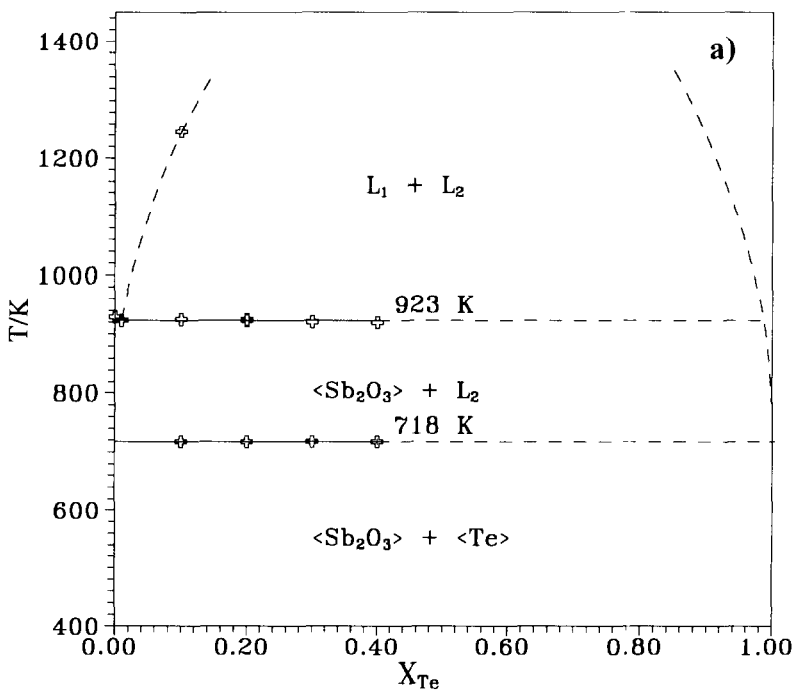

Fig. 10. Schematic representation of pseudobinary cross-sections: (a) Te–Sb_2O_3; (b) Te–Sb_2O_4; (c) Te–Sb_2O_3/Sb_2O_4 (1:1).

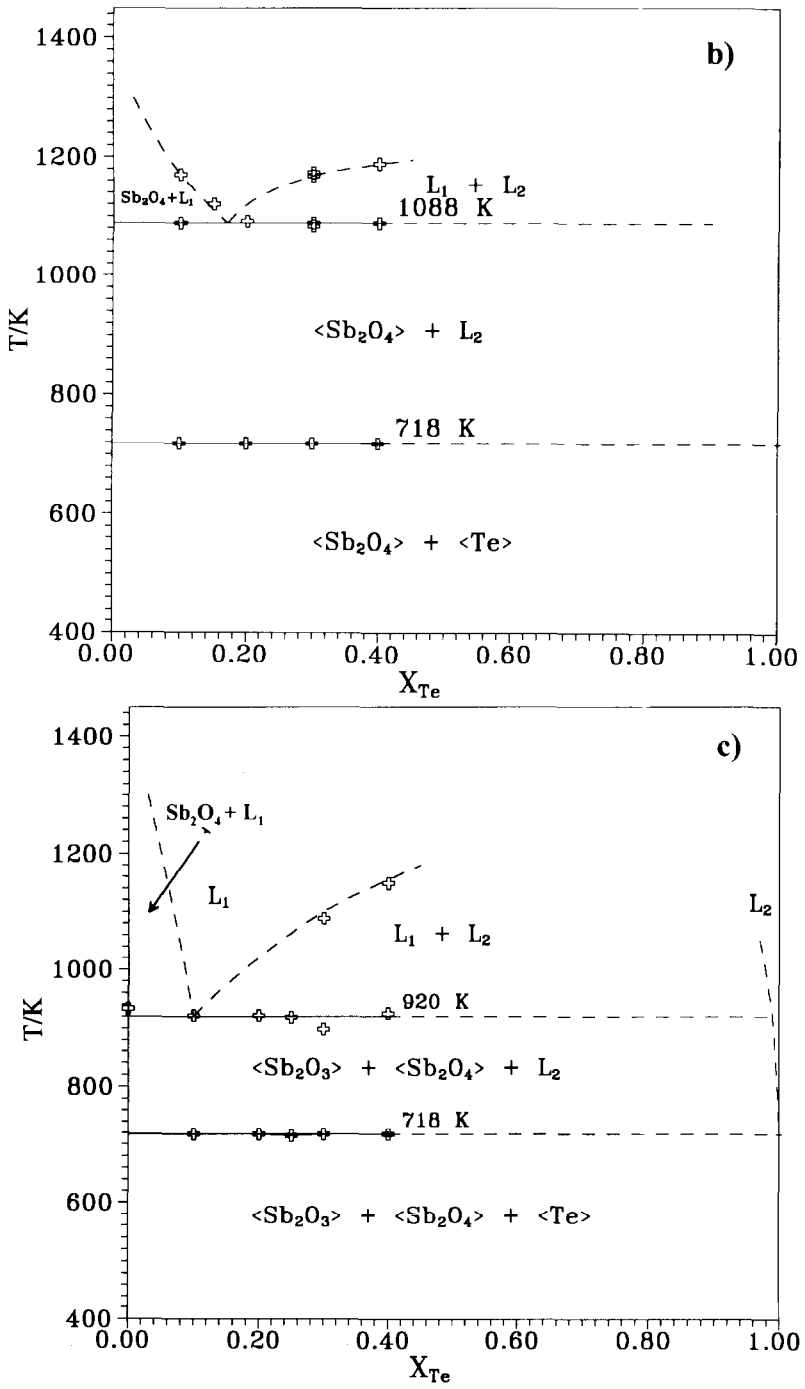

Fig. 10 *(continued)*

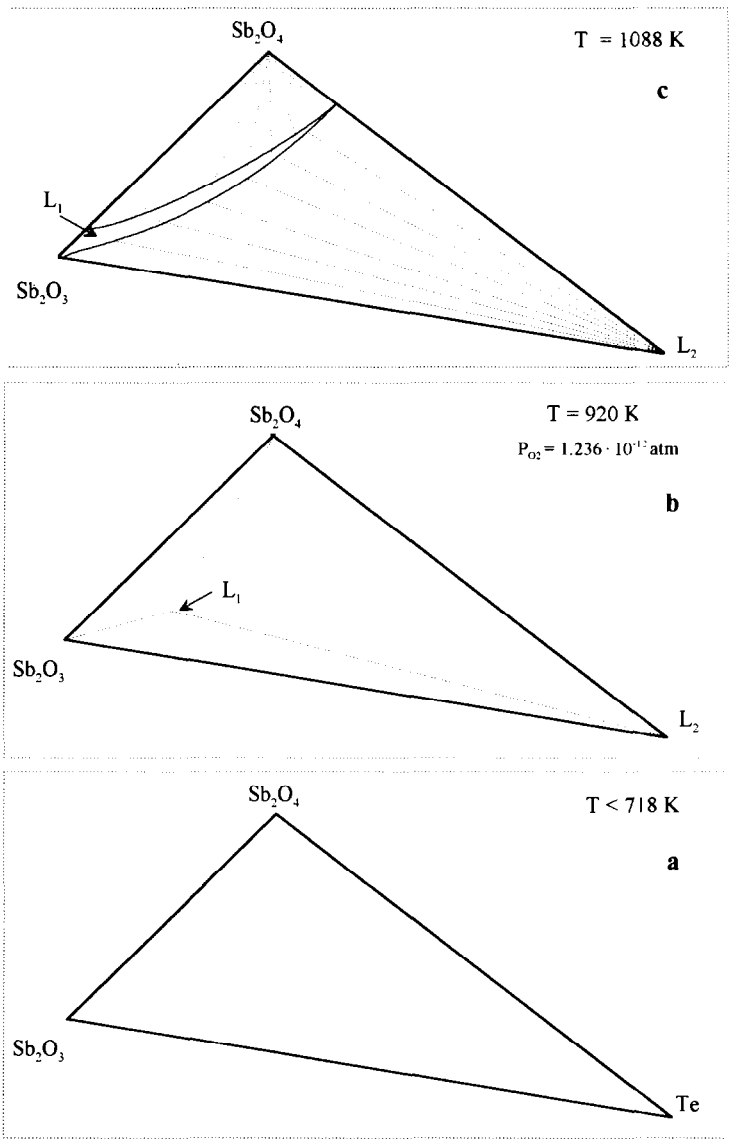

Fig. 11. Schematic representation of phase equilibria in the pseudoternary system: (a) below 718 K; (b) at 920 K; (c) at 1088 K.

3.4. *DTA determination of pseudobinary systems*

Three pseudobinary cross-sections namely, Te–Sb_2O_3, Te–Sb_2O_3:Sb_2O_4 (1:1), and Te–Sb_2O_4 of the ternary systems were examined by DTA measurements. Samples of approximately 0.2 g were prepared from pure components and were sealed under

vacuum in small silica vessels in order to contain the high vapour pressure of these components. Next, the silica vessels (Fig. 9) were placed in a DTA apparatus (Paulik, Paulik and Erdey, model OD-102, Hungary). Measurements were carried out in the temperature range 600–1300 K. The results obtained are presented in Figs. 10(a–c) for compositions up to 40 at% of tellurium. Two characteristic features can be noticed: at 718 K, a ternary eutectic (L_2) appears, which corresponds to almost pure liquid Te; at 920 K, another liquid (L_1) appears in the system.

Based on these results, the evolution of the pseudoternary system with temperature is suggested in Fig. 11(a–c). Liquid oxide phase (L_1) is formed at 920 K and remains at this temperature in equilibrium with (L_2) and both oxides. The formation of this phase can be described by the ternary four-phase equilibrium

$$L_2 + Sb_2O_4(s) + Sb_2O_3(s) = L_1 \tag{10}$$

Oxygen pressure in this ternary field can be calculated from the e.m.f. of cell III as

$$\log(p_{O_2})/\text{atm} = -\frac{21215.4}{T} + 11.1522 \tag{11}$$

yielding the value $p_{O_2} = 1.236 \times 10^{-12}$ atm at 920 K. Unfortunately, we did not manage to determine the composition of this point. It can be suggested, however, that it must be close to pure Sb_2O_3.

4. Discussion

In order to check the performance of our cell arrangement, we first determined $\Delta G^0_{f,TeO_2}$, which is known accurately form previous measurements [7–9]. Values of $\Delta G^0_{f,TeO_2}$ derived from e.m.f.s of cell I were found to be almost identical to those obtained by Chatterji and Smith [8] and very close to results of Otsuka and Kozuka [9] and Mallika and Sreedharan [7]. This fact speaks for the reliability of our cell performance while observed small differences can be attributed to different electric lead wires (graphite in Ref. [7] and Pt in Ref. [9]) used in the experiments. By combining our expression obtained for $\Delta G^0_{f,TeO_2}$ with that determined previously for oxygen dissolution in liquid tellurium, $\Delta G^0_{O(Te)}$ [5], we were able to calculate the saturation solubility limit and to suggest the Te-rich part of the Te–O phase diagram.

For the Sb_2O_3–Sb_2O_4 system, we found only two e.m.f. studies which provided $\Delta G^0_{f,Sb_2O_4}$, namely, those of Pankajavalli and Sreedharan [11], and Knauth and Schwitzgebel [15] who used solid oxide galvanic cells with zirconia electrolyte. Because the cell resistance increases significantly with falling temperature, Knauth and Switzgebel measured $\Delta G^0_{f,Sb_2O_4}$ at a constant temperature of 873 K only. In turn, Pankajavalli and Sreedharan added Pt powder into the mixture of oxides in order to enhance the electrical conductivity of the system. However, it was demonstrated by Kleykamp [10] that, up to 790 K, platinum oxide can be formed in oxygen or air and consequently, the e.m.f. of the cell can be changed due to this reaction.

Thus, we added Te to the working electrode which, on the hand, enhanced the conductivity of the cell and, on the other, is practically insoluble in solid antimony

oxides. It was observed that at low temperature the performance of cell III was much better than of cell II and consequently $\Delta G^0_{f,Sb_2O_4}$ was determined from measured e.m.f.s of cell III. Results were found to be almost identical with tabelaric values of Barin et al. [12], Kulikov [13] and Pankratz [14] which are based on calorimetric measurements.

Cell III worked well until liquid oxide phase appeared in the system. The condition of the formation of this phase can be determined by combining DTA measurements with p_{O_2} calculated from e.m.f.s of cell III (as given by Eq. (11)). It can be suggested that in the temperature range between 718 and 920 K only three phases, L_2, Sb_2O_3 and Sb_2O_4, exist. At 920 K, a four-phase reaction takes place

$$L_2 + Sb_2O_4(s) + Sb_2O_3(s) = L_1 \tag{12}$$

resulting in the formation of another liquid phase, L_1. At this particular temperature, 920 K, a ternary four-phase equilibrium occurs. The corresponding p_{O_2} pressure is given by relationship (11) and is equal to 1.236×10^{-12} atm.

Above 920 K, three-phase regions, L_1–$Sb_2O_4(s)$–L_2, L_2–L_1–$Sb_2O_3(s)$ and $Sb_2O_3(s)$–L_1–$Sb_2O_4(s)$, should exist. However, since the available information on the Sb_2O_3–Te cross-section as well as on the Sb_2O_3–Sb_2O_4 eutectic temperature suggests, that the field available for Sb_2O_3 crystallization is very small, it can be suggested that the composition of L_1 at 920 K is close to pure Sb_2O_3. Unfortunately, we were not able to verify this composition experimentally.

Acknowledgement

This work was supported by the State Committee for Scientific Research under Grant No. 308 669 101.

References

[1] L.A. Demina, S.L. Buzhak, V.A. Dolgikh, I.A. Khodyakova, B.A. Popovkin and A.V. Novoselova, Russ. J. Inorg. Chem., 26(3) (1981) 418.
[2] L.A. Demina, V.A. Dolgikh, S.L. Buzhak, B.A. Popovkin and A.V. Novoselova, Zh. Neorg. Khim. 26(5) (1981) 1434.
[3] E.A. Buketov, L.I. Mekler, E.G. Nadirov, A.S. Pashinkin and L.D. Trofimova, Zh. Neorg. Khim., 9 (1964) 224.
[4] T.B. Massalski, H. Okamoto, P.R. Subramanian and L. Kacprzak, Binary Alloys Phase Diagrams, Vol. 3, 2nd edn., ASM International, Materials Park, OH, 1990.
[5] B. Onderka, K. Fitzner and C.B. Alcock, in P. Danckwerts (Ed.), Symposium: High Temperature Materials Chemistry, The Institute of Materials, London, 1995, p. 163.
[6] B. Onderka and K. Fitzner, Z. Metallkd., 86(5) (1995) 313.
[7] C. Mallika and O.M. Sreedharan, J. Chem. Thermodyn. 18 (1986) 727.
[8] D. Chatterji and J.V. Smith, J. Electrochem. Soc., 120(7) (1973) 889.
[9] S. Otsuka and Z. Kozuka, Met. Trans., 11B (1981) 119.
[10] H. Kleykamp, Ber. Bunsenges. Phys. Chem., 87 (1983) 777.
[11] R.M. Pankajavalli and O.M. Sreedharan, J. Mater. Sci., 22 (1987) 177.

[12] I. Barin, O. Knacke and O. Kubaschewski, Thermochemical Properties of Inorganic Substances, Supplement, Springer-Verlag, Berlin, 1977.
[13] I.S. Kulikov, Thermodinamika Oksidov, Spravochnik. Izd. Metallurgia, Moskva, 1986.
[14] L.B. Pankratz, Thermodynamic Properties of Elements and Oxides, Bulletin 672, US Department of the Interior, Bureau of Mines, Washington D.C., 1982, p. 359.
[15] P. Knauth and G. Schwitzgebel, Ber. Bunsenges. Phys. Chem., 92 (1988) 32.